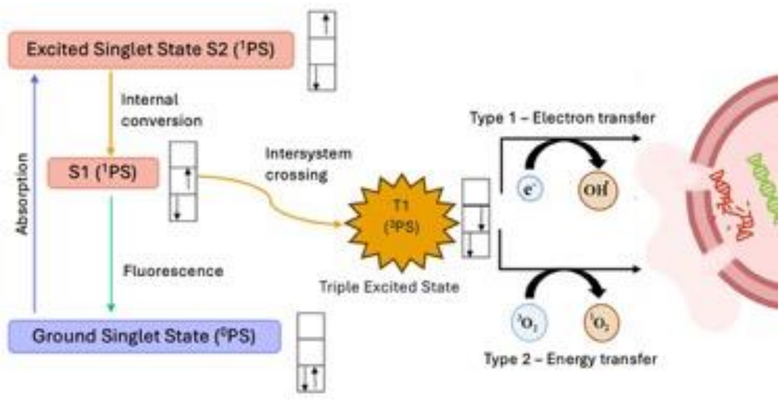
Evaluation of Curcumin and Its Derivatives as Photosensitizers for Antibacterial Photodynamic Therapy

Dafnomili Sofia[1], Lego Erika[1], Sagnou Marina[1,2], Christodoulakis Ioannis[1], Kythreoti Georgia[1]
[1] Deree-The American College of Greece, Department of Science and Mathematics, Gravias 6, 15342 Athens, Greece
[2] National Centre for Scientific Research "Demokritos", Institute of Biosciences and Applications, Patriarchou Gregoriou, 15310 Athens, Greece

Introduction

Antimicrobial resistance (AMR) is a growing global health threat, with over 1.27 million deaths attributed to drug-resistant infections in 2019 [1]. Antimicrobial photodynamic therapy (aPDT) offers a promising non-antibiotic alternative that combines a photosensitizer (PS), visible light, and molecular oxygen to generate reactive oxygen species (ROS) that kill bacteria [2]. Curcumin, a natural polyphenol from turmeric, shows potential as a PS due to its ROS-generating capacity under blue light. However, limitations such as poor solubility, photoinstability, and low affinity for bacterial membranes reduce its clinical utility [3]. This project explores whether chemical modifications to curcumin can enhance its antibacterial aPDT activity. aPDT involves excitation of the PS to a higher energy state, followed by intersystem crossing to a triplet state. From there, ROS can be generated either through electron transfer (Type I) or energy transfer to molecular oxygen (Type II), ultimately leading to generation of ROS that ultimately damage microbial structures, including membranes, proteins, and nucleic acids, resulting in cell death [4]. This project investigates whether curcumin analogues can be structurally optimized to improve their antibacterial aPDT activity.

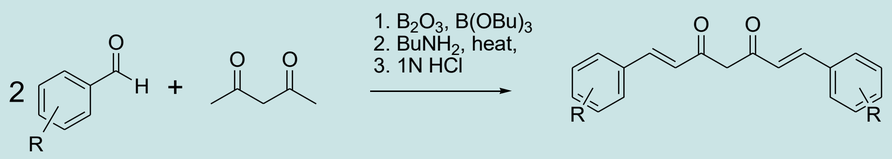
Figure 1
Jablonski Diagram: The Photochemical Mechanism of Action in Antimicrobial Photodynamic Therapy



Methodology

Compounds were synthesized via a three-step Pabon-based method involving boron-mediated protection of 2,4-pentanedione, aldol condensation with substituted benzaldehydes, and deprotection. Designed analogues aimed to enhance solubility, photostability, and light absorption. Syntheses were conducted in collaboration with NCSR "Demokritos."

Figure 2
General Synthetic Route for Curcumin Analogues



Photophysical characterization was performed using UV-Vis spectroscopy (300–700 nm) in DMSO to evaluate light absorption properties. Photodynamic activity was tested by exposing treated samples (0.3 mM to 0.0012 mM) to a 470 nm blue LED for 3 hours at an intensity of ~10 mW/cm². Controls for dark, light-only, DMSO vehicle, and ampicillin. Dark toxicity was determined via CFU assays on *E. coli* plated with compound (0.3 mM to 10 mM) in the absence of light. Bacterial growth was measured after 16–18 h incubation at 37 °C by OD_{600}, and IC_{50} values were calculated from sigmoidal dose–response curves.

Conclusions

- Most compounds exhibited minimal toxicity in the dark, confirming that antimicrobial effects were light-dependent.
- Structural modifications of curcumin (**C1**) significantly influenced photophysical and antibacterial properties. Removal of methoxy groups (**C2**, **C3**) modestly impacted efficacy, while full methylation (**C4**) diminished activity.
- C3 showed the lowest IC_{50} against S. aureus but exhibited an irregular dose–response, possibly due to solubility or aggregation effects.
- π-conjugation extension (**C5**, **C6**) resulted in broader, red-shifted absorption spectra, as expected, confirming successful spectral tuning for aPDT activation at longer wavelengths.
- However, red-shifted analogues did not consistently improve antibacterial activity, suggesting that light absorption alone is not sufficient — membrane affinity, cellular uptake, and ROS yield likely play critical roles.
- P. aeruginosa was generally more resistant, except for **C6**, which showed activity comparable to curcumin, indicating potential for selective application.
- Dose–response behavior and IC_{50} data suggest **C1** (curcumin) remains a reliable reference PS, with analogues offering target-specific improvements rather than broad-spectrum enhancement.
- Future design should focus on balancing photophysical properties with biological delivery factors, possibly through targeted delivery or conjugation strategies.

Acknowledgements

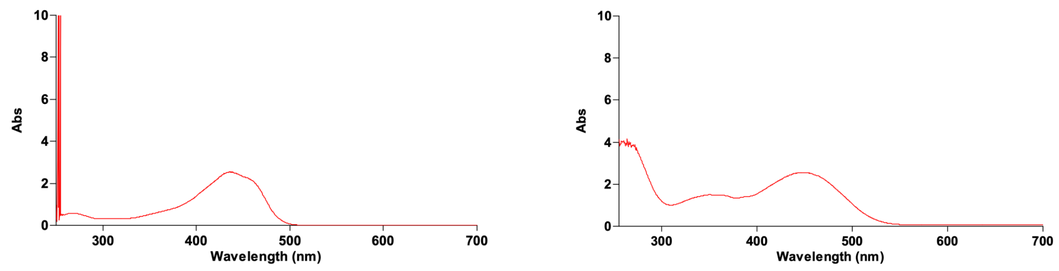
This project was supported by the Department of Science and Mathematics of Deree – The American College of Greece who funded this project and NCSR "Demokritos", where all compound were synthesized.

References

1. Sirwan, K. A., et al., *Journal of Medicine Surgery and Public Health,* **2024.**, 100081–100081.
2. Lima, E., & et al., *Molecules*, **2023,** 28(13), 5092.
3. Wang, X., et al., *Frontiers in Immunology*, **2023,** 14.
4. Zhang, C., et al., *National Science Review*, **2024,** 11(9).

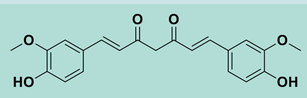
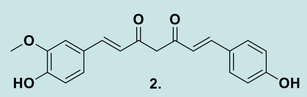
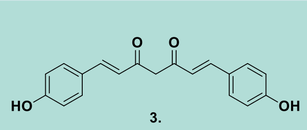
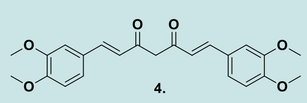
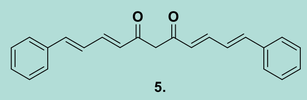
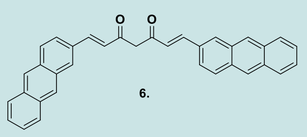
Results

Figure 3
Absorption Spectrum for Compounds C1 and C6



Absorption spectra of curcumin (**C1**) and the anthracene-substituted derivative (**C6**). **C1** shows a sharp peak at ~430 nm, while **C6** exhibits a broader, red-shifted band extending beyond 470 nm, consistent with enhanced π-conjugation and deeper light penetration potential. This spectral shift was the intended outcome of our molecular design to enable activation at clinically relevant wavelengths.

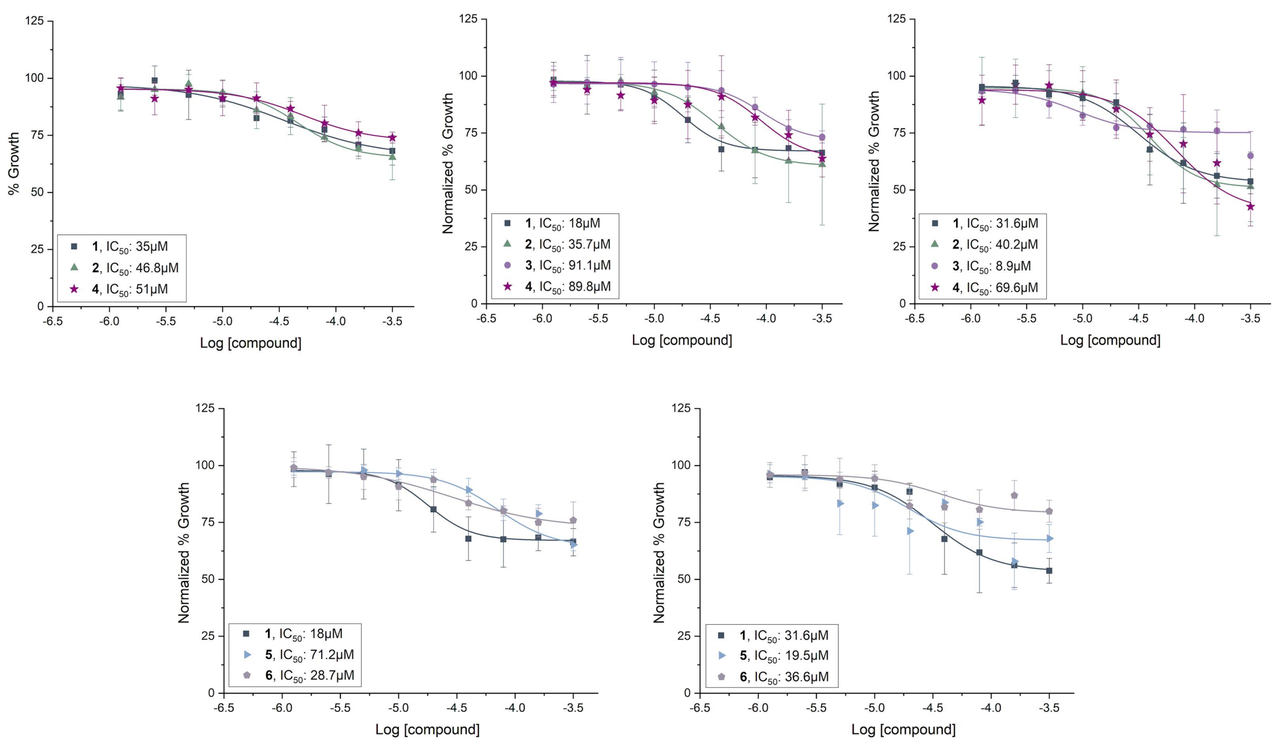
Figure 4
Comparative Summary of Curcumin and Analogues in Photodynamic Efficacy

Compound number/name	*Structure*	*Differences*	*E.coli*	*P. aeruginosa*	*S. aureus*
C1 curcumin	 1.		IC_{50}: 35μM E_{max}=70% R^2: 0.99994	IC_{50}: 18μM E_{max}=67% R^2: 0. 99987	IC_{50}: 31.6μM E_{max}=55% R^2: 0. 99994
C2 (1E,6E)-1-(4-hydroxy-3-methoxyphenyl)-7-(4-hydroxyphenyl) hepta-1,6-diene-3,5-dione	 2.	No methoxy on ring 2	IC_{50}: 46.8μM E_{max}=67% R^2: 0.99977	Non-ir. *linear IC_{50}: 35.7μM E_{max}=62% R^2: 0.99993	IC_{50}: 40.2μM E_{max}=53% R^2: 0. 99991
C3 (1E,6E)-1,7-bis(4-hydroxyphenyl)hepta-1,6-diene-3,5-dione	 3.	No methoxy groups	IC_{50}: 18.5μM E_{max}=87% *Almost Linear R^2: 0.99967	IC_{50}: 91.1μM E_{max}=75% R^2: 0.99999	IC_{50}: 8.9μM E_{max}=80% Cons. inactive R^2: 0. 99987
C4 (1E,6E)-1,7-bis(3,4-dimethoxyphenyl)hepta-1,6-diene-3,5-dione	 4.	All methoxy groups	IC_{50}: 51μM E_{max}=77% R^2: 0.99995	IC_{50}: 89.8μM E_{max}=64% R^2: 0.99977	IC_{50}: 69.6μM E_{max}=44% R^2: 0.99918
C5 (1E,3E,8E,10E)-1,11-diphenylundeca-1,3,8,10-tetraene-5,7-dione	 5.	Extended chain, no substitutions on the rings	*Linear R^2: 0.94791	IC_{50}: 71.2μM E_{max}=64% R^2: 0.99989	IC_{50}: 19.5μM E_{max}=60% R^2: 0.99955
C6 (1E,6E)-1,7-di(anthracen-2-yl)hepta-1,6-diene-3,5-dione	 6.	No extension, three rings in a series	*Linear R^2: 0.04488	IC_{50}: 28.7μM E_{max}=78% R^2: 0.99996	IC_{50}: 36.6μM E_{max}=80% Cons. inactive R^2: 0.99853

*inactive

This table presents the structural differences and photodynamic antibacterial activity of curcumin (**C1**) and its five analogues (**C2–C6**). Key metrics include IC_{50} values, E_{max} (maximum inhibition), and R^2 (fit quality) across three bacterial strains (*E. coli, P. aeruginosa, S. aureus*).

Figure 5
Dose Response Curves of Selected Analogues



Dose Response curves of analogues as compared to **curcumin** (**C1**). **A**. *E. coli* percent growth after treatment with activated **C1**, **C2** and **C4** (active). **B**. *P. aeruginosa* and **C**. *S. aureus* percent growth after treatment with activated **C1**, **C2** , **C3** and **C4**. **D**. *P. aeruginosa* and **E**. *S. aureus* percent growth after treatment with activated **C1**, **C5** , and **C6**.

IC_{50} values are also presented. These data illustrate how structural modifications affect bacterial susceptibility, with native **curcumin** (**C1**) performing consistently across all species, while π-extended analogues showed selective or diminished efficacy.